Structural and Dynamic Properties of Partially Charged Poly(acrylic acid) Gels: Nonergodicity and Inhomogeneities

Abdellatif Moussaïd† and Sauveur J. Candau

Laboratoire d'Ultrasons et de Dynamique de Fluides Complexes, Université Louis Pasteur, 4 rue Blaise Pascal, 67070 Strasbourg Cedex, France

Jacques G. H. Joosten*

Department for Physical & Analytical Chemistry, DSM Research, P.O. Box 18, 6160 MD Geleen, The Netherlands

Received September 24, 1993; Revised Manuscript Received January 13, 1994®

ABSTRACT: Small-angle neutron scattering (SANS) and light scattering experiments have been performed on partially neutralized poly(acrylic acid) (PAA) solutions and swollen networks with various cross-link densities. The ensemble-averaged intensity of light scattered from gels was measured by a procedure that allows the scanning of many independent speckles across the detector. For all investigated samples, the scattered light intensity was found to be independent of the scattering wave vector **q** in contrast with the behavior observed in neutral gels. SANS shows a peak in the structure factor, revealing the existence of microstructure at a small scale (~100 Å). The dynamic structure factors were obtained by using a method based on a recent theory of dynamic light scattering by nonergodic media. The PAA gels showed an increasingly nonergodic behavior upon an increase of cross-link content and/or a decrease of ionization degree. Light scattering and SANS results can be explained by assuming a liquid-like structure of densified clusters.

I. Introduction

In recent years, the effect of the nonergodicity of solid-like media like colloidal glasses[1,2] or polymeric gels[3–9] on dynamic light scattering (DLS) measurements has attracted a great deal of attention. In a polymeric gel, the polymer segments are restricted by the cross-links to particular regions of the sample and are only able to perform limited Brownian motion about fixed average positions. As a result, one particular sample of a gel is trapped in a restricted region of phase space defined by its average configuration and the extent of the fluctuations about this configuration. A gel may thus be regarded as a nonergodic medium since a time-averaged measurement on a particular sample will not, in general, be equivalent to an ensemble-averaged measurement, i.e., one averaged over a representative number of all possible spatial configurations. A recent theory of DLS by nonergodic media developed by Pusey and van Megen[9] provides a method to extract from time-averaged intensity correlation function (ICF) measurements the normalized dynamic structure factor $f(q,t)$ associated with polymer concentration fluctuations and more specifically allows a measure of the fraction of frozen-in fluctuations resulting from constrained motion of the polymeric segments. This theory was used and checked by Joosten et al. in a study of the diffusional behavior of polystyrene latex spheres incorporated in polyacrylamide gels.[3]

The dynamical structure factor of pure polyacrylamide gels was also determined using the same method,[4] and it was shown that, at high cross-link density or high total monomer concentration, there is a large contribution from frozen-in fluctuations, showing clear evidence of nonergodic behavior. However, in the latter case, the interpretation of the measurements is more complex due to the existence of large-scale imperfections in the network structure that have a spatial extent or correlation range comparable to the wavelength of the light.[10–15]

As a result, the ensemble-averaged intensity of light scattered by the gel is much stronger than by a solution of the same concentration and is dependent on scattering vector q. By combining DLS and static light scattering experiments (SLS), the fluctuating part of the scattered light can be separated from the total scattered intensity. It was found in polyacrylamide gels that this fluctuating part is q independent and slightly larger for gels than for polymer solutions at the same concentration.[4] Also the mobility of the polymer chains was found to be larger than in analogous solutions.[4] This suggests that the ICF from polyacrylamide gels can be treated as suggested in earlier studies[10,15–18] in terms of a heterodyne mixing between large-scale static inhomogeneities and the dynamic field associated with long-wavelength dynamic density fluctuations of the same nature as in polymer solutions, i.e., quasi-ergodic. On the one hand, this viewpoint then implies that one considers the large-scale inhomogeneities as some irrelevant objects in the system. On the other hand, one knows that these objects constitute an intrinsic part of the gel systems. This problem is still waiting for a definite and more satisfying answer.

From experiments performed by Moussaïd et al.[8] on charged poly(acrylic acid) (PAA) it was shown that gels show little or no excess scattering compared to the equivalent solutions. Measured time- and ensemble-averaged intensity correlation functions for these systems are almost identical, implying the absence of nonergodic features. Furthermore, the first cumulant as obtained from the initial decay of the ICF was found to be about the same in the gel and in the solution at the same polymer concentration. Small-angle neutron scattering (SANS) experiments were also performed on these PAA gels. The structure factor was found to have a peak at finite wave vector q^*, revealing the existence of a microstructure at very small scale (~100 Å) in the gels.[19–22] The results obtained were well understood in the framework of recent theoretical studies[23,24] in which it is shown that such materials are liable to form mesophases at a microscopic scale.

† Current address: Department for Physical & Analytical Chemistry, DSM Research, P.O. Box 18, 6160 MD Geleen, The Netherlands.

® Abstract published in *Advance ACS Abstracts*, March 1, 1994.

0024-9297/94/2227-2102$04.50/0

The purpose of this paper is to take advantage of the homogeneity of the weakly ionized PAA gels at the scale of the wavelength of the light to thoroughly investigate possible nonergodic effects associated with the presence of the cross-links. To this end we use the fact that the PAA gels do not exhibit angle-dependent light scattering intensity. In the study by Moussaïd et al.,[8] only gels with relatively low cross-link densities have been investigated. In this paper we present results of both SANS and DLS in weakly ionized PAA gels with various cross-linking degrees.

The paper is organized as follows: in section II the relevant notions and equations for the analysis of DLS measurements in nonergodic media are summarized. Section III gives the theoretical background necessary for the analysis of the SANS data relative to the structure factor of weakly charged polyions having an amphiphilic character due to a poor solubility of the backbone in water.[23,24] Section IV deals with the experimental details, and here we present some experimental results on systems that are obtained by copolymerizing acrylic acid and methylenebisacrylamide. The total monomer content of the gel is kept constant at 0.707 M (5 wt %), whereas both the cross-link content and the ionization degree are varied, the latter by addition of sodium hydroxide. Section V is devoted to a discussion of the results in view of the theory of DLS by nonergodic media and of the model developed for the density–density correlation function of weakly ionized systems. We find that the gels under study show an increasingly nonergodic behavior upon an increase of the cross-link content and/or a decrease of the ionization degree. The above results are likely to be associated with a change of the microscopic structure of the gels as the scattering is found to increase in the whole q range (both in light and neutron experiments) with, however, the remarkable result that the scattered intensity of light remains q independent, which indicates the absence of inhomogeneities at the scale of the wavelength of the light.

II. Dynamic Light Scattering from Nonergodic Media: Theoretical Background

In this section only a survey of the expressions directly relevant to the discussion of DLS on gels is given. For a rigorous treatment and a thorough theoretical discussion of DLS experiments on nonergodic media, see the paper by Pusey and van Megen.[9]

DLS measures the time-averaged time correlation function of the intensity $I(q,t)$ of light scattered by the sample in the direction described by the scattering vector $\mathbf{q}$, $|\mathbf{q}| = (4\pi/\lambda)\sin(\theta/2)$, λ and θ being the wavelength of the light and the scattering angle in the medium, respectively. This intensity is proportional to $|\rho(q,t)|^2$, where $\rho(q,t)$ is the qth spatial Fourier component of the fluctuations causing the scattering. The normalized ensemble-averaged density–density correlation function (or intermediate scattering function (ISF)) $f(q,\tau)$ is given by

$$f(q,\tau) = \frac{\langle \rho(q,0)\rho^*(q,\tau)\rangle_E}{\langle |\rho(q)|^2\rangle_E} \quad (1)$$

where τ denotes time and the subscript E indicates an ensemble average over all possible configurations of the medium.

For an arbitrary nonergodic medium the amplitude $E(q,t)$ ($\sim\rho(q,t)$) of the scattered field at the detector can be written as the sum of two components[9]

$$E(q,t) = E_F(q,t) + E_c(q) \quad (2)$$

where the fluctuating component $E_F(q,t)$ is a zero-mean complex Gaussian variable and $E_c(q)$ is a constant (time-independent) field. When the gel is regarded as an arbitrary nonergodic medium, the constant field is that arising from the "frozen-in" density fluctuations.[9] The time-averaged statistical properties of the fluctuating component $E_F(q,t)$ of the field scattered by a particular volume of the sample can be written in terms of full ensemble averages;[9] i.e.

$$\langle E_F(q,0)E_F^*(q,\tau)\rangle_T = \langle E_F(q,0)E_F^*(q,\tau)\rangle_E = \langle I(q)\rangle_E[f(q,\tau) - f(q,\infty)] \quad (3)$$

where $\langle\ldots\rangle_T$ indicates a time average. The zero-time limit of eq 3 gives

$$\langle I_F(q)\rangle_T = \langle I(q)\rangle_E[1 - f(q,\infty)] \quad (4)$$

where $f(q,\infty)$ is the limiting value of $f(q,\tau)$ for $\tau \to \infty$.

A single DLS measurement provides an estimate of $g_T^{(2)}(q,\tau)$, the normalized time-averaged time correlation function of the scattered intensity

$$g_T^{(2)}(q,\tau) \equiv \frac{\langle I(q,0)I(q,\tau)\rangle_T}{\langle I(q,0)\rangle_T^2} \quad (5)$$

where the intensity is given by $I(q,t) = |E(q,t)|^2$. In ref 9 a procedure is presented for calculating $f(q,\tau)$ from $g_T^{(2)}(q,\tau)$ when the system under study exhibits nonergodic behavior. In this paper we follow only the so-called "brute force" method for determining $f(q,\tau)$; i.e., we determine the ensemble-averaged intensity–intensity correlation function by a procedure described in ref 4. This approach provides an estimate of $g_E^{(2)}(q,\tau)$, the normalized ensemble-averaged time correlation function of the scattered intensity, defined as

$$g_E^{(2)}(q,\tau) \equiv \frac{\langle I(q,0)I(q,\tau)\rangle_E}{\langle I(q,0)\rangle_E^2} \quad (6)$$

By using the well-known (Siegert) relation, we calculate the intermediate scattering function from $g_E^{(2)}(q,\tau)$

$$g_E^{(2)}(q,\tau) = 1 + |\beta f(q,\tau)|^2 \quad (7)$$

where β is the spatial coherence factor which depends largely on the number of coherence areas seen by the detector.[5,6]

A comparison of the results for $f(q,\tau)$ as obtained by using either $g_T^{(2)}(q,\tau)$ or $g_E^{(2)}(q,\tau)$ can be found in refs 4 and 7.

III. Weakly Charged Polyelectrolyte Systems: Theoretical Background

It has been shown recently that a semidilute solution of a weakly charged polyelectrolyte in a poor solvent undergoes a mesophase separation transition by lowering the temperature, provided the salt concentration is low enough.[23,24] This mesophase consists of oppositely charged polymer dense and polymer dilute regions arranged in a periodic array. The free-energy increase due to the local violation of the electroneutrality condition is compensated by the gain of entropy for the counterions.

Near the Θ condition, i.e., when the solvent is marginal with respect to the backbone of neutral monomers, even though there may be no permanent mesoscopic segregation, some finite wavelength monomer concentration fluctua-

tions are enhanced, leading to a peak in the structure factor $S(q)$. Assuming the polymer chains to remain nearly Gaussian, the structure factor for the solution reads

$$S(q) = \frac{1}{4\pi l_B r_0^2 \alpha^2} \frac{q^2 r_0^2 + s}{(q^2 r_0^2 + s) + (q^2 r_0^2 + t) + 1} \quad (8)$$

where l_B is the Bjerrum length, α is the fraction of ionized monomers, and r_0 is a typical distance given by

$$r_0^{-2} = \left(\frac{48\pi l_B}{a^2}\right)^{1/2} \alpha \varphi^{1/2} \quad (9)$$

where α is the length of the monomer unit and φ is the number of monomers per unit volume ($\sim$polymer concentration). The parameter s is a reduced ionic strength defined as $s = \kappa^2 r_0^2$, where κ^{-1} is the usual Debye–Hückel screening length, and t is a reduced temperature given by $t = -12\, r^2 h\varphi/a^2$, where $h = -(2v\tau + 3w\varphi)$ is the usual virial term in a Θ solvent, v being the excluded volume, $\tau = (T - \Theta)/\Theta$ the reduced temperature, and w the third virial coefficient.

In a limited range of polymer concentration φ, ionization degree α, and salt concentration φ_s, the structure factor (eq 8) exhibits a maximum for a nonzero value q^* of the wave vector transfer, given by

$$q^{*2} + \kappa^2 = r_0^{-2} \quad (10)$$

and in the limit of large scattering wave vectors, eq 8 predicts a q^{-2} decay of the scattering intensity which is consistent with the assumption that the chains remain Gaussian and can be treated within the RPA formalism.

The scattered intensity $I(q)$ is related to the structure factor $S(q)$ by $I(q) = K^2 S(q)$, where K is the contrast factor related to the diffusion lengths of the monomer and of the solvent.

The above model, although it is meant for semidilute solutions, has been used to interpret the SANS results obtained in cross-linked PAA networks.[19,20] Indeed, a peak was observed in the structure factor of these systems. The variations of the peak position and amplitude with ionization degree, salt content, and temperature were found to be in qualitative agreement with the theoretical predictions.

The dynamics of concentration fluctuations of a weakly charged polyelectrolyte semidilute solution have also been studied theoretically and experimentally in the limit where they are controlled by hydrodynamic interactions.[26] Three relaxation modes were found: a plasmon mode corresponding to the fast relaxation of charge fluctuations, a diffusive mode involving mainly the motion of the small ions to restore the Donnan equilibrium, and a slower cooperative diffusion mode corresponding to the breathing motion of the polyelectrolyte chains and ions. It is the last mode that is probed by DLS in the low-q regime. The associated cooperative diffusion coefficient D_c can be calculated analytically but leads to a rather complex form. In the limit where the electrostatic effects dominate the excluded volume interactions, it is given by[20,26]

$$D_c = \frac{k_B T}{6\pi\eta}\left(\frac{\beta^3}{\kappa^2}\right)\left(1 + \frac{\kappa^2}{\beta^2}\right)\left(2 + \frac{\kappa^2}{\beta^2}\right)^{-1/2} \quad (11)$$

where the length $1/\beta = [a^2/48\pi l_B \alpha^2 \varphi]^{1/4}$.

The variation of D_c with ionization degree, salt content, and polymer concentration for PAA gels with relatively small cross-link content was found to be qualitatively described by eq 11.[20]

IV. Experimental Section

A. Materials. The solutions of poly(acrylic acid) were prepared by radical polymerization of acrylic acid in aqueous solution. Gels were obtained by radical copolymerization of acrylic acid and methylenebisacrylamide. All reactions were initiated by ammonium peroxydisulfate in the reaction bath. The polymer concentration C_p was kept constant and equal to 0.707 M. The degree of cross-linking R_c is defined as the monomer ratio methylenebisacrylamide/acrylic acid.

The degree of ionization α of PAA is defined as the ratio of carboxylate groups to the total number of monomers. PAA is a weak acid, and the ionization degree can be varied over a very wide range by changing the pH of the medium. In aqueous solution, α has a nonzero value due to the acid–base equilibrium

$$-(CH_2CH(COOH))- + H_2O \rightleftarrows -(CH_2CH(COO^-))- + H_3O^+$$

We have approximated the dissociation constant with that of the monomeric acrylic acid: $K_a = 5.6 \times 10^{-5}$. This leads to a value of $\alpha = 0.9 \times 10^{-2}$ for $C_p = 0.707$ M.

High ionization degrees ($\alpha > 10^{-2}$) were obtained by addition of NaOH to the solution to partially neutralize the polyacid to a given stoichiometric ionization degree according to

$$-(CH_2CH(COOH))- + Na^+OH^- \rightleftarrows -(CH_2CH(COO^-))- + H_2O + Na^+$$

This leads to an ionic strength $I \equiv \alpha$, due to Na^+ counterions.

A standard procedure was used to prepare the samples.[8,21] The solution was filtered with a 0.2-μm filter to get rid of dust particles. A few milliliters was then poured into a light scattering cell. Nitrogen was bubbled in the solution to remove the dissolved oxygen which would inhibit the radical reaction. The reaction was carried out in an oven at 70 °C during 8 h. Samples for SANS experiments were prepared along the same lines but with replacement of H_2O by D_2O to obtain a good contrast.

B. Experimental Setup and Methods. SANS. SANS experiments were performed on the PACE spectrometer in the Laboratoire Léon Brillouin (Laboratoire commun CEA–CNRS). The sets of experiments were performed under the same conditions: $\lambda \approx 5.4$ Å for the wavelength of the incident neutrons and a sample–detector distance equal to 3 m. This configuration allows one to obtain q values in the range $(1.15 \times 10^{-2} < q\ (\text{Å}^{-1}) < 1.22 \times 10^{-1})$.

All data were treated according to standard procedures for small-angle isotropic scattering. The spectra were corrected for transmission, sample thickness, and electronic noise. Monomer solutions with the same composition as those used to prepare gels were taken as background samples. This approach enables a correct estimate of the contribution of incoherent scattering. In particular, the transmission of the monomer solutions is within 1.5%, of the polymer samples. Normalization to the unit incident flux, determination of geometrical factors, and detector cell efficiency corrections were performed by using the incoherent scattering of H_2O, corrected for the scattering of the empty cell. The data were put on an absolute scale by introducing the value $d\Sigma/d\Omega \approx 0.86$ cm^{-1} for the differential incoherent scattering of H_2O at 25 °C. This absolute scattering intensity $I(q)$ is directly proportional to the structure factor $S(q)$ that is calculated theoretically (eq 8).

Light Scattering. Light scattering measurements were accomplished by using the apparatus and methods described in ref 4. In summary, the instrument comprises an ALV/SP-86 goniometer (ALV, Langen, Germany) equipped with an Ar^+ laser (Coherent, Innova 90) operating at an output power of $\approx$400 mW. The incident beam (wavelength in vacuo $\lambda_0 = 514.5$ nm) is polarized vertically with respect to the scattering plane. A Glan-Thompson prism is used for detecting only vertically polarized scattered light. Intensity correlation functions (ICF's) were measured by an ALV-3000 or an ALV-5000 multibit correlator (ALV, Langen, Germany). The correlators yield a

$g_T^{(2)}(q,\tau)$ that consists of 192 (ALV-3000) or 256 (ALV-5000) logarithmically spaced channels allowing a time span of nine decades in one run. A stepping motor used in conjunction with the correlator allowed ensemble-averaged correlation functions, $g_E^{(2)}(q,\tau)$, to be collected in a semiautomated fashion. In these measurements the stepping motor, attached to the sample, turns a random number of steps and then stops, and the correlator starts collecting data for a certain period (typically, 5–10 min). When the correlator is finished, the motor again turns a random number of steps, and the correlator is restarted without clearing the memory. This procedure is repeated a large number of times (typically, 50–100), the data being accumulated in the correlator channels. Then the total correlation function data are read from the correlator and normalized by the total number of photon counts and the number of summations, thereby using the built-in option of symmetrical normalization. From this ensemble-averaged intensity correlation function, an intermediate scattering function was calculated by using the well-known (Siegert) relation, eq 7.

As will be described, the scattered intensity $\langle I(q)\rangle_T$ at a particular scattering angle varies strongly when scanning through various positions in the sample (see Figure 2). Therefore, methods were developed that enabled, an estimation of $\langle I(q)\rangle_E$ and a determination of the properties of $\langle I(q)\rangle_T$.[3,4]

The automated procedure for determining the ensemble-averaged intensity, $\langle I(q)\rangle_E$, was as follows: the count rate was measured for 15 s during which the cylindrical sample cell was continuously rotated by the stepping motor at a speed of 30 rpm. This measurement was repeated ten times at each scattering angle, and $\langle I(q)\rangle_E$ was taken as the average count rate. Although relative intensities were obtained accurately, we did not measure absolute scattering cross sections.

The properties of $\langle I(q)\rangle_T$ were studied by measuring the probability distribution ($P(\langle I(q)\rangle_T)$). In this experiment the count rate for a particular speckle[36] was recorded using an integration time of 15 s; then the sample was rotated a random number of steps and then stopped, and the count rate was again measured. This whole process was repeated up to 500–1000 times for a given sample and scattering angle.

SANS Experiments. In Figure 1 the structure factors as obtained from SANS experiments for PAA gels with ionization degrees equal to 0.9×10^{-2}, 2.2×10^{-2}, and 5.1×10^{-2} respectively and at various cross-linking degrees are depicted. For small degrees of cross-linking, the structure factor is the same as for solutions of the same concentration if one excepts a small enhancement of the scattering. As the cross-linking degree increases, the amplitude of the peak increases and its position is shifted toward the low-q region. Eventually the peaks move outside the q range explored by SANS experiments. It can also be noted that the scattering is reduced upon an increase of α, in accord with the theoretical prediction of eq 8 and previous experimental data.[19-21] Table 1 gives the values obtained for the peak position q^*, the amplitude of the peak $I(q^*)$, and the exponent characteristic of the asymptotic behavior of $S(q)$ in the high-q regime. One can remark that the relative increase of $I(q^*)$ with R_c is enhanced upon an increase of the cross-link content.

SLS Experiments. Using the method described in section IVB for scanning through various positions in the sample, we have determined the probability distribution of the time-averaged intensity $P(\langle I\rangle_T)$. A typical result is shown in Figure 2 for a sample with $\alpha = 0.022$ and $R_c = 0.005$ at a scattering angle $\theta = 50°$. The histogram represented in this figure is constructed by grouping the data in intervals of kcounts/s, resulting in an estimate of the probability distribution function $P(\langle I(q)\rangle_T)$ of the scattered intensity, $\langle I(q)\rangle_T$, sampled over the full ensemble. The probability distribution function shows a cutoff at low intensities resulting from the contribution $\langle I_F(q)\rangle_T$, the average of the fluctuating component. In addition to this, one observes a negative exponential part, characteristic for nonergodic behavior resulting from $I_c(q)$ (see eq 2). It is shown that[3]

$$P(\langle I(q)\rangle_T) \sim H(\langle I(q)\rangle_T - \langle I_F(q)\rangle_T) \exp\left[-\frac{\langle I(q)\rangle_T - \langle I_F(q)\rangle_T}{\langle I(q)\rangle_E - \langle I_F(q)\rangle_T}\right] \quad (12)$$

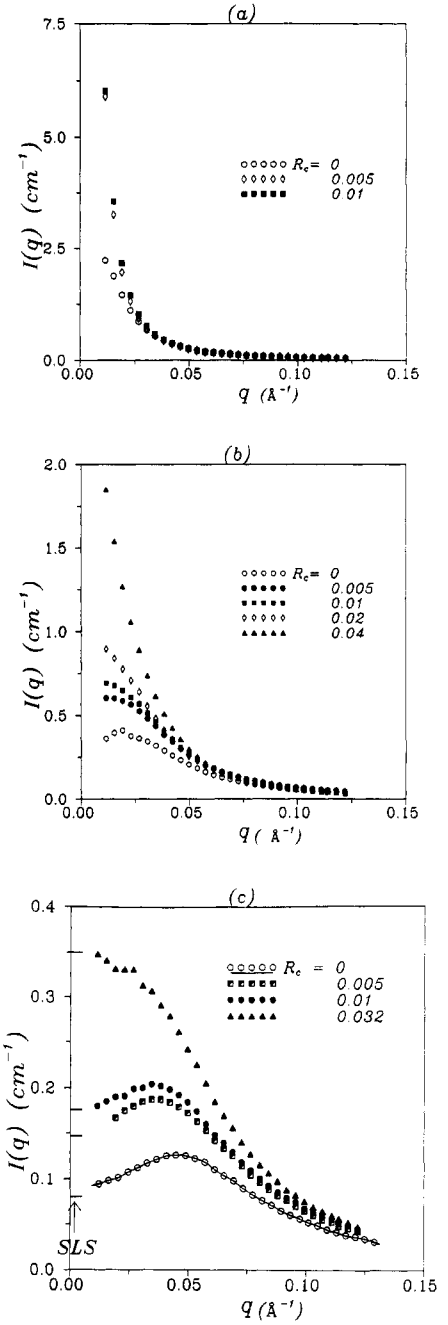

Figure 1. Scattered intensity from PAA gels (C_p = 0.707 M) with ionization degree $\alpha = 0.9 \times 10^{-2}$ (a), $\alpha = 2.2 \times 10^{-2}$ (b), and $\alpha = 5.1 \times 10^{-2}$ (c) at various cross-linking degrees. The solid line in (c) is the best fit of eq 8 to the experimental structure factor; the values of the three free parameters are K = 8 b, a = 9 Å, and h = 13 Å^3 (see ref 21).

Table 1. Characteristics of the Samples Studied by SANS

sample	C_p (M)	α	R_c	κ^2 (Å^{-2})	q^* (Å^{-1})	$I(q^*)$	exponent
S500	0.707	0.009	0	3.44×10^{-3}			1.9
G500	0.707	0.009	0	3.44×10^{-3}			2.05
S502	0.707	0.022	0	8.98×10^{-3}	0.019	0.45	2.06
G502	0.707	0.022	0.005	8.98×10^{-3}	0.015[a]	0.70[a]	2
G502R2	0.707	0.022	0.01	8.98×10^{-3}	0.012[a]	0.79[a]	2.16
G502R3	0.707	0.022	0.02	8.98×10^{-3}			2.15
G502R4	0.707	0.022	0.04	8.98×10^{-3}			2.67
S505	0.707	0.051	0	1.98×10^{-2}	0.044	0.178	1.9
G505	0.707	0.051	0.005	1.98×10^{-2}	0.037	0.226	2
G505R2	0.707	0.051	0.01	1.98×10^{-2}	0.034	0.245	2.04
G505R3	0.707	0.051	0.032	1.98×10^{-2}			2.25

[a] Values estimated from the fit of $S(q)$ to eq 8.

where $H(x)$ is the Heaviside function; $H(x) = 0$ for $x < 0$ and $H(x) = 1$ for $x > 0$.

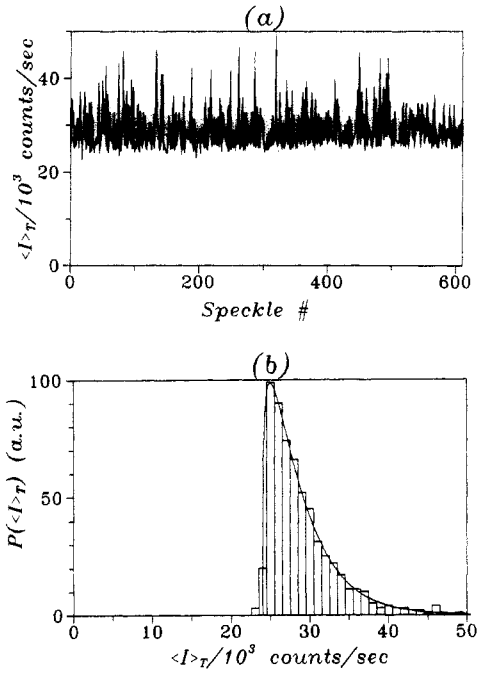

Figure 2. (a) $\langle I(q)\rangle_T$ for various speckles as obtained by scanning various positions in the sample (C_p = 0.707 M, α = 0.022, R_c = 0.005) at a scattering angle θ = 50°. (b) Frequency distribution $P(\langle I(q)\rangle_T)$ of the data given in (a); the solid line is the least-squares fit of eq 12.

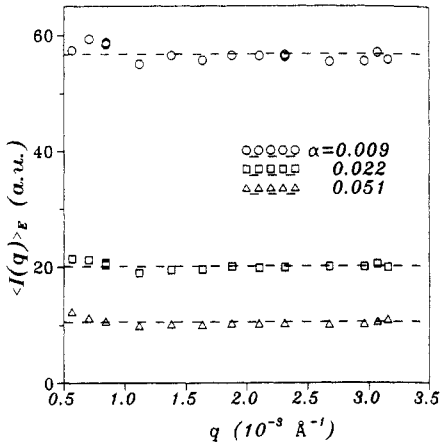

Figure 3. Variation of the ensemble-averaged scattered intensity versus scattering vector for PAA at various ionization degrees (R_c = 0.005).

In deriving eq 12 it is assumed that the integration time for measuring $\langle I(q)\rangle_T$ is chosen such that it comprises many typical decay times of the fast fluctuations in the system. The solid line in Figure 2b is a nonlinear least-squares fit of the function given in eq 12 to the data. One notices that the data are well described by this function, which implies that the scattered field $E(q,\tau)$ associated with this intensity is a zero-mean Gaussian stochastic variable when sampled over the full ensemble. From the parameters used to construct the curve in Figure 2b we find $\langle I_F(q)\rangle_T$ = 18 kcounts/s and $\langle I(q)\rangle_E$ = 22 kcounts/s when corrected for scattering volume; the procedure, described in section IVB, for obtaining $\langle I(q)\rangle_E$ gives the same value within experimental error (±5%).

The ratio $\langle I\rangle_E/\langle I\rangle_F$ is found to be significantly smaller than for polyacrylamide gels. It tends toward 1 as the ionization degree is increased, showing a less and less pronounced nonergodic behavior. By using eq 4, we find $f(q,\infty)$ = 0.18 from these data. This value agrees very well with the result we obtain for $f(q,\infty)$ from the analysis of ensemble-averaged ICF's to be described below.

Figures 3 and 4 illustrate the effects of respectively the ionization degree and the cross-link content on the ensemble-averaged intensity. It is seen that, contrary to what is observed

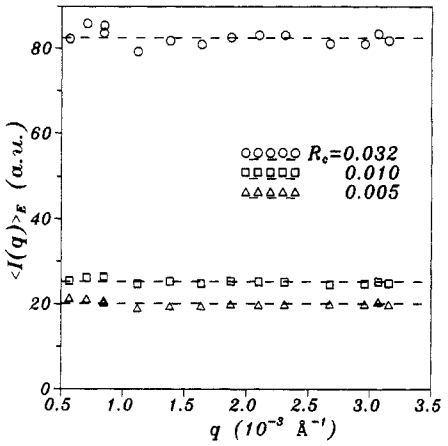

Figure 4. Variation of the ensemble-averaged scattered intensity versus scattering vector for PAA at various cross-link contents (α = 0.022).

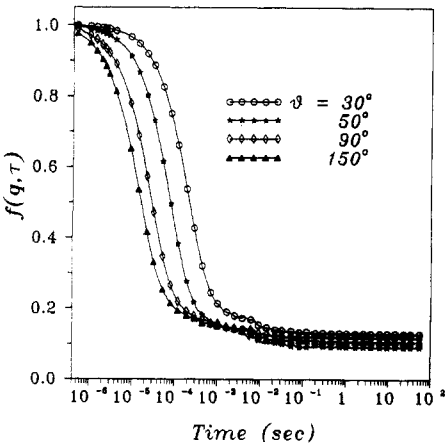

Figure 5. Angle dependence of intermediate scattering function $f(q,\tau)$ for PAA gel with R_c = 0.005 and α = 0.022.

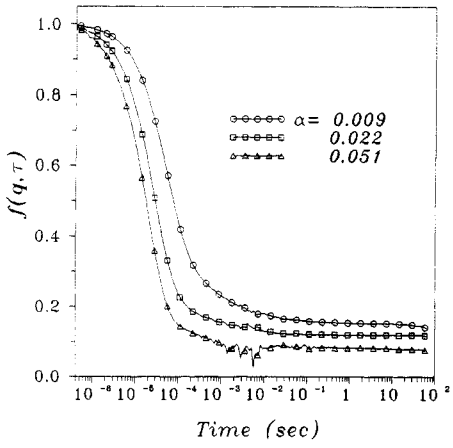

Figure 6. Intermediate scattering functions $f(q,\tau)$ for PAA gels at various ionization degrees (R_c = 0.005, θ = 90°).

in neutral gels, $\langle I\rangle_E$ is independent of q. Moreover, it decreases upon an increase of α and/or a decrease of R_c, in agreement with previous measurements.[8]

DLS Experiments. The ensemble-averaged ICF $g_E^{(2)}(q,\tau)$ were constructed by using the procedure described in section IVB from unnormalized ICF's of 100 different speckles requiring a measuring time of ~5 h. To obtain the dynamic structure factor $f(q,\tau)$ from $g_E^{(2)}(q,\tau)$, we use eq 7. Figure 5 shows the dynamic structure factors for a gel with α = 0.022 and R_c = 0.005 at different scattering vectors q. One observes that $f(q,\tau)$ decays to a finite value, $f(q,\infty)$, for $\tau \to \infty$, characteristic of nonergodic behavior. It can be seen in Figure 5 that there is no significant angular dependence of $f(q,\infty)$. Figures 6 and 7 show the effects of respectively α and R_c on the dynamic structure factor $f(q,\tau)$.

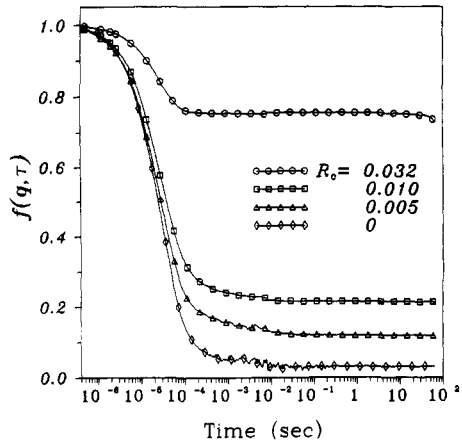

Figure 7. Intermediate scattering functions $f(q,\tau)$ for PAA systems at various cross-link contents ($\alpha = 0.022$, $\theta = 90°$).

Table 2. Characteristics of the Samples Studied by SLS and DLS

sample	R_c	α	$\langle I\rangle_E$	$\langle I_F\rangle_E$	$f(q,\infty)$	D_c (10^{-7} cm^2 s^{-1})
S500	0	0.009	42	42		3.1
G500	0.005	0.009	56	48	0.14	2.4
S502	0	0.022	15	15		6.2
G502	0.005	0.022	20	17.6	0.12	5.4
G502R2	0.01	0.022	25	18.6	0.24	4.5
G502R3	0.032	0.022	83	21.6	0.74	1.8
S505	0	0.051	8.4	8.4		9.6
G505	0.05	0.051	10	9.2	0.08	8.6

It can be seen that $f(q,\infty)$, which is a measure of the frozen-in density fluctuations, increases upon a decrease of α and/or an increase of R_c. It is also obvious from Figure 7 that the gels show a larger $f(q,\infty)$ than the equivalent solution.

Using eq 4, one can, by combining SLS and DLS experiments, determine the intensity $\langle I_F\rangle_T$ ($=\langle I_F\rangle_E$) of the fluctuating component.

Table 2 summarizes the results obtained for $\langle I\rangle_E$, $\langle I_F\rangle_T$, and $f(q,\infty)$. Also reported in Table 2 are the values for the first cumulant $\langle\Gamma\rangle/q^2$ ($=D_c$) as obtained from the initial slope of $f(q,\tau)$.

V. Discussion

Concerning the shape of the structure factor, it is seen in Figure 1c that, for cross-linked samples with $\alpha = 0.051$, there are still some finite wavelength concentration fluctuations that are enhanced. Only the position and the amplitude of the peak are modified. In fact, eq 8 still fits the data, provided one uses an "effective" length of the monomeric unit increasing with the cross-link density. This indicates clearly that the cross-linked gel is reminiscent of the fluctuations occurring in semidilute solutions. This is found also for samples with lower ionization degree, as seen in Figure 8, which represents $c/I(q)$ versus q^2 for the systems with $\alpha = 0.022$ (c_p is the polymer concentration in g/g). In the low-q regime one can observe an upward curvature, contrary to the case of semidilute solutions of neutral polymers, where $c/I(q)$ is a linear function of q^2, and that of the neutral gels, where generally a downward curvature is observed.[10] The difference of behavior of neutral and ionized gels is also evidenced by the light scattering experiments, which lead to a q-independent ensemble-averaged intensity for the PAA gels investigated here.

The results of Figures 1 and 4 show a net enhancement of the scattering in the whole q range upon increasing the cross-link content. Such an effect cannot be totally attributed to an enhancement of the contrast factor resulting from the introduction in the medium of a new species, i.e., the methylenebisacrylamide. The latter contribution can be estimated from the analysis of the asymptotic behavior of $I(q)$ at large q. The Kratky plots

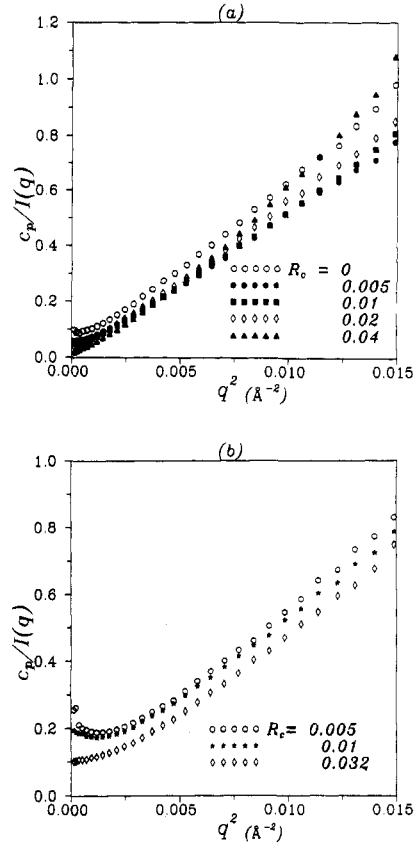

Figure 8. Plots of $c_p/I(q)$ versus q from PAA systems with ionization degree $\alpha = 0.022$ (a) and $\alpha = 0.051$ (b) at various cross-link contents.

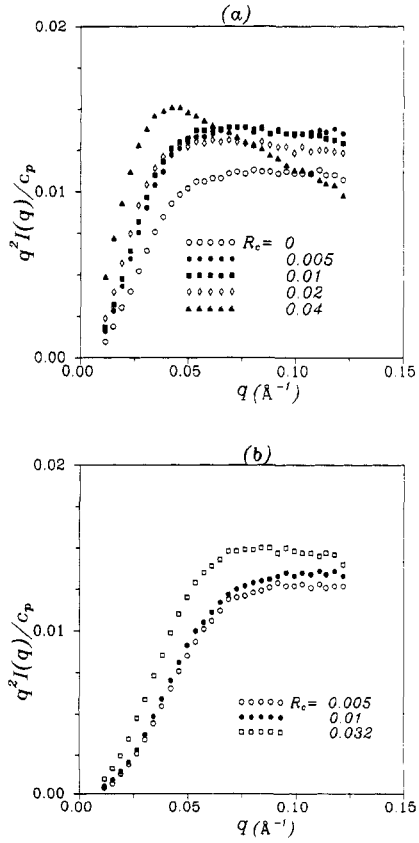

Figure 9. Kratky plots of the intensities scattered from PAA systems with ionization degree $\alpha = 0.022$ (a) and $\alpha = 0.051$ (b) at various cross-link contents.

of $q^2I(q)$ versus q^2 reported in Figure 9 show that an increase of R_c induces a slight increase of the contrast factor. Moreover, this large-q behavior is described by a

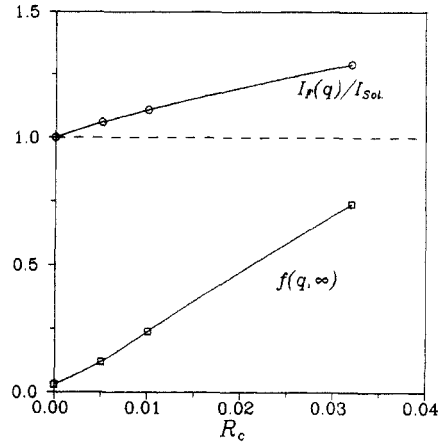

Figure 10. Effect of cross-link content R_c on the fluctuating component $I_F(q)$ and frozen-in component $f(q,\infty)$.

power law with an exponent close to 2, except the two samples with the highest cross-linking density (cf. Table 1). For the samples with $R_c = 0.032$ the contrast cannot be estimated since no plateau value is reached for $q^2I(q)$ in the high-q range.

A direct comparison of the SANS and light scattered intensities in the low-q range is not possible since we do not know precisely the contrast factor and also because light scattering experiments were performed in H_2O whereas SANS experiments used D_2O systems. However, to compare relative changes in magnitude, we have adjusted in Figure 1c the intensity of light scattered by the solution to the values obtained by fitting the SANS curve. The scattered intensities obtained by light scattering on the gel samples were then calculated using this reference. The results, reported in Figure 1c, are in reasonable agreement with the neutron scattering spectra.

The scattering results cannot be interpreted by assuming that the effect of the cross-links is simply to limit the spatial extent of the monomer concentration fluctuations without inducing any structural change. This would lead to an overall scattered intensity independent of R_c in the first approximation as this intensity is essentially controlled by the entropy of the counterions. The frozen-in contribution $f(q,\infty)$ should increase with R_c but at the expense of the fluctuating component I_F. Here, we observe a behavior similar to that of neutral gels,[4] i.e., an increase of both $f(q,\infty)$ and, to a much smaller extent, I_f (cf. Figure 10), which suggests that a structural change occurs with formation of microdomains with size much smaller than the wavelength of the light.

To interpret the structural changes brought about by the cross-linking of weakly charged polymers, it was suggested by Briber et al.[27] and by Shibayama et al.[28] to use the approach developed by de Gennes[29] for gels formed by a mixture of two incompatible linear polymers. The de Gennes model predicts a structure factor with exactly the same shape as that given by eq 8. Indeed eq 8 describes well the SANS data that we have obtained in cross-linked gels. However, in the de Gennes model the position of the peak q^* varies like $N_x^{-1/2}$, where N_x is the degree of polymerization between cross-links. Therefore an increase of cross-linked density should shift the peak of the structure factor toward larger q values, the opposite of the trend seen in our experiments.

Alternatively, we can tentatively propose the following scheme: in the first stages of the polymerization process, branched macromolecules are formed. As soon as they are long enough that a semidilute regime is established, enhanced fluctuations occur with a characteristic wave vector q^* that depends on α and, to a lesser extent, on C_p (cf. eq 8). It can then be conjectured that the unreacted methylenebisacrylamide, which is hydrophobic, and the more branched polymers already formed tend to localize in the polymer-dense regions, leading to a microscopic spinodal decomposition in the gel. These effects are well described by the Flory theory of polymer solutions.[30]

According to the above scheme, the system in the limit of high R_c can be envisioned as a liquid-like assembly of dense beads. The intensity scattered by such a system is given by[31]

$$I(q) \sim NV^2S(q)\,P(q) \tag{13}$$

where N is the number of "particles", V is the volume occupied by one particle, $S(q)$ is the structure factor representing the interparticle interferences, and $P(q)$ is the intraparticle interference. Since we observe no angular dependence of light scattered intensity (Figures 3 and 4), we can approximate $P(q) \approx 1$.

If we assume that the total mass ($\sim NV$) of the "beads" (dense microdomains) remains constant upon varying the cross-link density, then the observed increase of $I(q\to 0)$ with R_c would reflect an increase of the bead size ($I(q\to 0) \sim V$). On the other hand, it is known experimentally[32] that, in concentrated colloidal dispersion, the particles are held by the repulsive interactions at mean equidistant positions that fill the whole volume. This means that if the volume of the "beads" is increased by an increase of R_c, at constant mass NV, then q^* should vary as $V^{-1/3}$ and therefore as $I(q=0)^{-1/3}$. The results of Figure 1c (see also Table 1) are consistent with this approximation.

In addition to the enhancement of the scattering and the shift of q^* toward lower q values as R_c increases, we observe also an increase of the absolute value of the asymptotic exponent (cf. Table 1 and Figure 9) that might be indicative of more dense polymer domains.

The dynamic properties can also be analyzed within the framework of the above schematic picture. On the basis of this model (see Figure 11), one can envisage three sources of fluctuations: fluctuations due to the polymer chains inside the "beads", those connecting the "beads", and those due to the "beads" themselves. The data relative to the diffusion coefficient $D(q)$ reported in Table 2 and in Figure 12 have been obtained by regarding the sample as arbitrary nonergodic media. Thus $D(q)$ describes the average decay of all fluctuations. At high R_c, the dominant contribution to the scattering comes from the "particles" (or beads) that are spatially localized as revealed by static experiments. We conjecture that the DLS experiments could be described by the model of a particle moving around its equilibrium position like a harmonically bound Brownian particle (HBP model).

For harmonically bound Brownian identical particles in identical environments $f(q,\tau)$ reads[1]

$$f(q,\tau) = \exp\left\{-q^2\langle\delta^2\rangle\left[1 - \exp\left(-\frac{Dq^2\tau}{q^2\langle\delta^2\rangle}\right)\right]\right\} \tag{14}$$

where $\langle\delta^2\rangle$ is one Cartesian component of the long-time mean-square displacement of a particle from its average position.

We used the latter equation for fitting the data given in Figure 13.

Although the HBP model seems to fit data reasonably well, the observed q independence of $f(q,\infty)$ (cf. Figure 5) is in conflict with this model (the HBP model predicts $f(q,\infty) = \exp(-q^2\langle\delta^2\rangle)$).

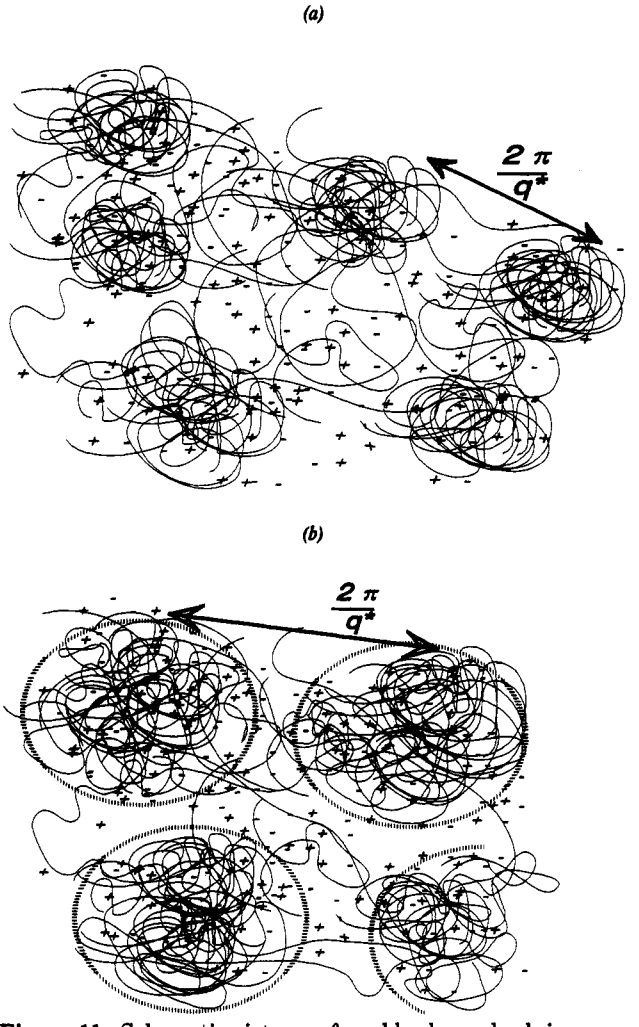

Figure 11. Schematic pictures of weakly charged gels in a poor solvent: (a) lower cross-link content; (b) higher cross-link content.

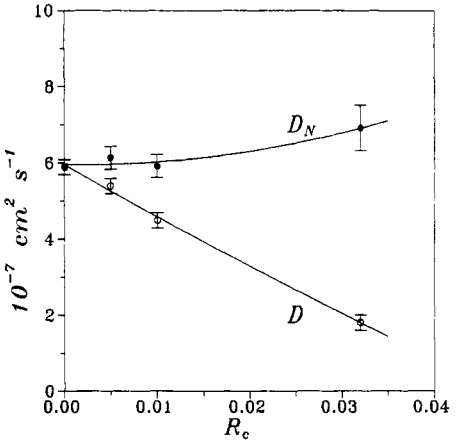

Figure 12. Variation of the diffusion coefficient for PAA systems versus cross-link content. $D(q)$ represents the average decay of all fluctuations. $D_N(q)$ is the diffusion coefficient associated with the dynamic fluctuations (heterodyne approach).

The other extreme case would be a model in which the relaxation phenomena result entirely from a "gel mode" of all polymer chains running through an essentially static assembly of particles. In this case one can define an intermediate scattering function associated with the relevant dynamic component of the density fluctuations of the network by[4]

$$f_N(q,\tau) = \frac{\langle E_F(q,0)E_F^*(q,\tau)\rangle_T}{\langle I_F(q)\rangle_T} \quad (15)$$

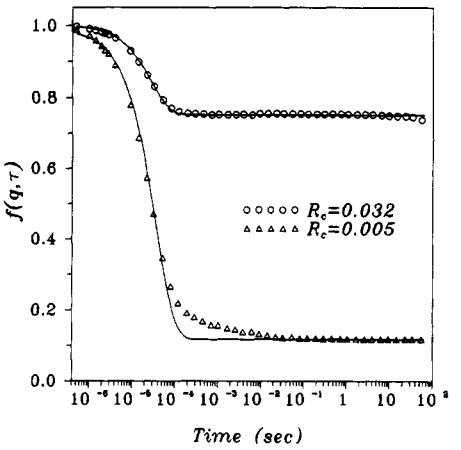

Figure 13. Effect of cross-link content R_c on the shape of $f(q,\tau)$ with $\alpha = 0.022$ and $\theta = 90°$. The solid line is an exponential fit to the decaying part of $f(q,\tau)$.

It was shown that the diffusion coefficient $D_N(q)$ describing the average decay of $f_N(q,\tau)$ is related to $D(q)$ by

$$D_N(q) = \frac{D(q)}{1 - f(q,\infty)} \quad (16)$$

The experimental values of D_N are essentially independent of the scattering vector, which fits into the picture that only long-wavelength fluctuations are observed. The variation of D_N with R_c is reported in Figure 12. The fact that, within experimental error, D_N is independent of R_c gives support to this approach.

Formally, one also obtains expressions 3 and 4 if the so-called heterodyne approach is used for interpreting DLS experiments.[4] In the heterodyne detection mode the light scattered by the dynamic density fluctuations is mixed with the scattering arising from a local oscillator. In the literature (see, e.g., ref 15) this local oscillator is assumed to be provided by the scattering from large-scale inhomogeneities in the sample. The resulting diffusion coefficient, which describes only the relaxation of the dynamic part of the density fluctuations, is interpreted in terms of a viscoelastic model of a gel, whereas in treating the gel as a general nonergodic medium, one inherently takes into account all the features of the gel. The diffusion coefficient $D(q)$ can be regarded as resulting from two relaxation processes: one having an amplitude $\{1 - f(q,\infty)\}$ and diffusion coefficient $D_N(q)$ and the other with an amplitude $f(q,\infty)$ and diffusion coefficient zero.

VI. Conclusion

The PAA gels are characterized by a periodic structure and no large-scale inhomogeneities, in contrast with the behavior observed in neutral gels; the frozen-in fluctuations increase upon a decrease of ionization degree α and/or an increase of cross-linking density R_c. Those observations come from the fact that the properties of weakly charged polyelectrolytes result from a subtle balance between hydrophobic and Coulombic interactions.

The structure of such gels is consistent with a model of a liquid-like assembly of beads. In the limit where a microphase separates into a two-phase structure with a sharp interface, one expects an exponent of -4 in $S(q)$ at large q. This indeed has been observed by Shibayama et al.[28] on weakly ionized copolymers, close to a phase transition.

An important point is the condition at which the gels are prepared. We observed that the fluctuations of

scattered intensity by poly(acrylic acid) (PAA), poly(methacrylic acid) (PMA), and polyacrylamide (PAM) depend strongly on the way the gels are prepared, the form of the phase diagram (if the system presents an upper critical solution temperature (UCST) or a lower critical solution temperature (LCST)), and the difference between the gelation temperature and Θ point.[33] A similar result was observed in the case of neutral gels by Suzuki et al.[34]

Given the results, one could point out that the microscopic structure of polymer gels is a superposition of two components (fluctuating and frozen-in). The dynamic fluctuations are alternatively the same for the gel and solution. The presence of cross-links is responsible for the formation of a substructure of quasi-static dense microdomains. Such substructures strongly influence the properties of gels.[11,14] The hypothesis of "uninteresting" large-scale inhomogeneities, which has been used,[16-18] is without justification. (It could be justified in the case of the presence of dust particles, due to the setup and/or the workers but not to the system itself.)

To conclude, we mention that there is still no microscopic theory for the intermediate scattering function $f(q,t)$ of a gel. Recently, Slot et al.[35] showed that the nonergodic behavior of gels can be simulated. Such simulations can establish an important means to understand the topological structure of gels.

Acknowledgment. We thank J. P. Cotton and E. Geladé for useful assistance during experiments and for helpful discussions. We are also grateful to P. Pusey for his helpful suggestions. A.M. thanks J. P. Munch and F. Schosseler for many enlightening discussions.

References and Notes

(1) Pusey, P. N.; van Megen, W. *Phys. Rev. Lett.* **1987**, *59*, 2083.
(2) Pusey, P. N.; van Megen, W. *Ber. Bunsenges. Phys. Chem.* **1990**, *94*, 225.
(3) Joosten, J. G. H.; Geladé, E. T. F.; Pusey, P. N. *Phys. Rev. A* **1990**, *42*, 2161.
(4) Joosten, J. G. H.; McCarthy, J. L.; Pusey, P. N. *Macromolecules* **1991**, *24*, 6690.
(5) Jakeman, E. In *Photon Correlation and Light Beating Spectroscopy*; Cummins, H. Z., Pike, E. R., Eds.; Plenum Press: New York, **1974**; p 75.
(6) For our experimental setup β was determined to be 0.960 ± 0.005 using a standard polystyrene latex dispersion.
(7) Joosten, J. G. H. *Prog. Colloid Polym. Sci.* **1993**, *91*, 149.
(8) Moussaïd, A.; Munch, J. P.; Schosseler, F.; Candau, S. J. *J. Phys. II (Les Ulis, Fr.)* **1991**, *1*, 637.
(9) Pusey, P. N.; van Megen, W. *Physica A* **1989**, *157*, 705.
(10) Candau, S. J.; Bastide, J.; Delsanti, S. *Adv. Polym. Sci.* **1982**, *44*, 27.
(11) Weiss, N.; Van Vlet, T.; Silberberg, A. *J. Polym. Sci.* **1979**, *17*, 2229; **1981**, *19*, 1505.
(12) Stein, R. S. *J. Polym. Sci.* **1969**, *B7*, 657.
(13) Bastide, J.; Leibler, L. *Macromolecules* **1988**, *21*, 2647.
(14) Dusek, K.; Prins, W. *Adv. Polym. Sci.* **1969**, *6*, 1.
(15) Candau, S. J.; Joung, C. Y.; Tanaka, T.; Lemarechal, P.; Bastide, J. *J. Chem. Phys.* **1979**, *70*, 4694.
(16) Munch, J. P.; Candau, S.; Duplessix, R.; Picot, Cl.; Benoit, H. *J. Phys. Lett. Fr.* **1974**, *35*, 239.
(17) Geissler, E.; Hecht, A. M. *J. Chem. Phys.* **1976**, *65*, 103.
(18) Munch, J. P.; Candau, S.; Hild, G. *J. Polym. Sci., Polym. Phys. Ed.* **1977**, *15*, 11.
(19) Schosseler, F.; Ilmain, F.; Candau, S. J. *Macromolecules* **1991**, *24*, 225.
(20) Schosseler, F.; Moussaïd, A.; Munch, J. P.; Candau, S. J. *J. Phys. II (Les Ulis, Fr.)* **1991**, 1197.
(21) Moussaïd, A.; Schosseler, F.; Munch, J. P.; Candau, S. J. *J. Phys. II (Les Ulis, Fr.)* **1993**, *3*, 573.
(22) Candau, S. J.; Moussaïd, A.; Munch, J. P.; Schosseler, F. *Makromol. Chem., Macromol. Symp.* **1992**, *62*, 183.
(23) Borue, V.; Erukhimovich, I. *Macromolecules* **1988**, *21*, 3240.
(24) Joanny, J. F.; Leibler, L. *J. Phys. Fr.* **1990**, *51*, 545.
(25) Raphaël, E.; Joanny, J. F. *Europhys. Lett.* **1990**, *13*, 623.
(26) Adjari, A.; Leibler, L.; Joanny, J. F. *J. Chem. Phys.* **1991**, *95*, 4580.
(27) Briber, M.; Bauer, B. *J. Macromolecules* **1988**, *21*, 3296.
(28) Shibayama, M.; Tanaka, T.; Han, H. C. *J. Chem. Phys.* **1992**, *97*, 6842.
(29) de Gennes, P.-G. *J. Phys. Fr.* **1979**, *40*, L-60.
(30) de Gennes, P.-G. *Scaling Concepts in Polymer Physics*; Cornell University Press: Ithaca, NY, 1979.
(31) Riley, D. P.; Oster, G. *Discuss. Faraday Soc.* **1951**, *11*, 107.
(32) Vrij, A.; Nieuwenhuis, E. A.; Fijnault, H. M.; Agterof, W. P. M. *Discuss. Faraday Soc.* **1978**, *65*, 101.
(33) Moussaïd, A.; Joosten, J. G. H., to be published.
(34) Suzuki, Y.; Nozaki, K.; Yamamoto, T.; Itoh, K.; Nishio, I. *J. Chem. Phys.* **1992**, *97*, 3308.
(35) Slot, H.; Moussaïd, A.; Joosten, J. G. H., to be published.
(36) The illuminated volume is always much the same. On rotating the sample in different directions, different Fourier components or speckles are obtained.